

INDC International Nuclear Data Committee

Experimental Investigation of the Properties of Scission Neutrons In Thermal-Neutron Induced Fission of ^{233}U and ^{235}U

A.S. Vorobyev, O.A. Shcherbakov
Petersburg Nuclear Physics Institute of National Research Center
“Kurchatov Institute”, Gatchina, Russia

February 2020

Selected INDC documents may be downloaded in electronic form
from <http://nds.iaea.org/publications>
or sent as an e-mail attachment.

Requests for hardcopy or e-mail transmittal should be directed to
NDS.Contact-Point@iaea.org

or to:

Nuclear Data Section
International Atomic Energy Agency
Vienna International Centre
PO Box 100
1400 Vienna
Austria

Printed by the IAEA in Austria

February 2020

Experimental Investigation of the Properties of Scission Neutrons In Thermal-Neutron Induced Fission of ^{233}U and ^{235}U

A.S. Vorobyev, O.A. Shcherbakov
Petersburg Nuclear Physics Institute of National Research Center
“Kurchatov Institute”, Gatchina, Russia

ABSTRACT

The properties of “scission” neutrons from thermal neutron induced fission of ^{233}U and ^{235}U were obtained by comparing experimental angular and energy distributions of the prompt fission neutrons measured recently at PNPI with model distributions calculated under the assumption that all prompt fission neutrons are emitted from fully accelerated fragments. To obtain model distributions, it is assumed to use the spectra of prompt fission neutrons measured at small angles relative to the preferential direction of movement of light and heavy fragments because it is expected that just for these angles the contribution of non-primary mechanism is minimal while a contribution of neutrons emitted by complementary fragment can be taken into account correctly. It is also very important that in this approach it is possible to obtain the model distributions practically unlimited in low-energy range.

February 2020

Contents

Introduction	7
1. Description of the experimental set-up	10
2. Model	10
2.1. General.....	10
2.2. Analysis of PNPI's data	14
3. Results.....	16
3.1. Comparison of the PNPI's experimental results and model calculation.....	16
Conclusion.....	22
References	22
Appendix 1	25
Appendix 2	26
Appendix 3	27

Introduction

In spite of considerable progress has been achieved in studying nuclear fission at low excitation energies, there are still a number of questions that must be answered to gain better insight into this phenomenon. Among the things that still remain poorly studied are the nature and properties of transition states near the fission barrier, the mechanism for redistribution of the excitation energy of the fissioning nucleus between the fission fragments, and the interrelation between collective and single-particle oscillations during the evolution of the nucleus to the scission point.

A special attention deserves the question of the existence of scission neutrons emitted from fissioning nucleus during its evolution from equilibrium deformation to the scission point and thus carrying information about fission dynamics. The search for scission neutrons and investigations of their properties are complicated by impossibility of discriminating in an experiment between these neutrons and neutrons emitted from the fission fragments fully accelerated in the mutual Coulomb field. These investigations can only be conducted by comparing measured distributions of the prompt fission neutrons (PFNs) and model calculations performed by assuming that all PFNs are emitted from fully accelerated fragments. The estimates of the scission neutron yield based on the available experimental data show that the main PFN emission mechanism is the emission from fully accelerated fragments [1-8]. But for the detailed description of angular and energy distributions of PFNs, it is necessary to assume the existence of neutrons whose emission mechanism differs from evaporation of neutrons from fully accelerated fragments (emission of neutrons before or at the time of scission of a fissioning nucleus or in the process of acceleration of produced fission fragments), such neutrons are called as “scission” neutrons. Note that there is still no reliable information on the existence and properties of “scission” neutrons. In the best studied case of spontaneous fission of $^{252}\text{Cf}(\text{sf})$, the yield of “scission” neutrons varies from 1 to 20% of the total neutron yield per fission event (Fig.1, upper part) [8-22]. The available literature data on thermal neutron induced fission of ^{235}U are given in Table 1.

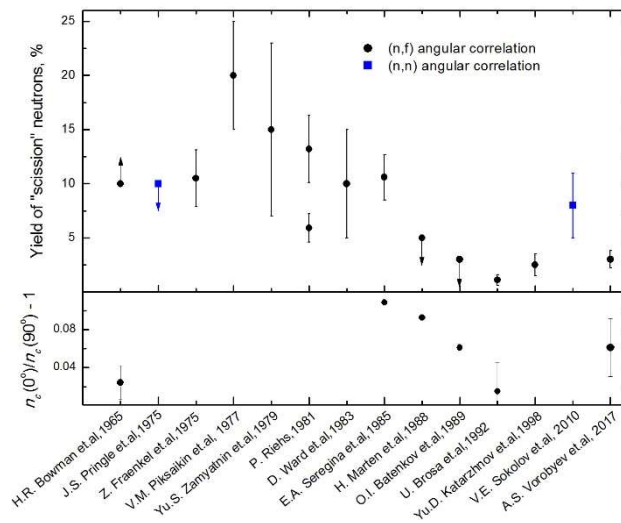


Fig. 1. Results of the investigations of PFN emission mechanism for spontaneous fission of ^{252}Cf (literature data): upper part – “scission” neutron yield (downward arrows – upper boundary, upward arrows – lower boundary), lower part – anisotropy of angular distribution of PFNs in the center-of-mass system of fission fragments.

Table 1. Main results of the investigations of neutron emission mechanism for $^{235}\text{U}(n,f)$.

Authors, References Experimental Set-up	Yield of “scission” neutrons	Average energy of “scission” neutrons	Anisotropy of PFN emission in the centre-of-mass system of fission fragment, A_2
<i>Investigation of (n,f)-angular correlation</i>			
<u>K. Skarsvag et.al. [4] (1963).</u> A gas scintillation counter with collimator was used as FFs detector; One neutron detector (plastic scintillator), TOF (90cm). The angle between the direction of FFs and neutrons was varied with 15° step by pivoting the FFs counter about an axis.	15%	~ 1.8 MeV	“There is a little or no indication of any anisotropy ...”
<u>S.S. Kapoor et.al. [6] (1963).</u> Ion chamber scintillation detector used for measuring FF angle and kinetic energy of fission fragment; One neutron detector (plastic scintillator), TOF(103cm).	10%	3.2 MeV	$\leq 0.09 \pm 0.06$ [5]
<u>J.S. Fraser et.al. [7] (1966).</u> Two plastic scint. for FFs spectroscopy (TOF with base 125cm and 99cm); Four neutron detectors (plastic scintillator) were used, TOF (106cm). The neutron spectra measurements were done simultaneously at 10° , 25° , 45° and 80° relative to FFs direction.	20%	1.9 MeV	“... all results are consistent with $A = 0.$ ”
<u>M.S. Samant et.al. [23] (1995).</u> IC used for FFs spectroscopy and measuring FF angle; One neutron detector (NE213), n/ γ pulse shape discrimination, TOF (70 cm).	$10 \pm 2\%$	---	Not investigated
<u>N.V.Kornilov et.al. [24] (2001).</u> Compilation of Skarsvag’s data [4].	15%	Two components with average energy 0.9 MeV and 3.0 MeV.	
<u>A.S. Vorobyev et.al. [25] (2010).</u> 16 MWPC for FFs spectroscopy (TOF with base 14cm); Two stilbene neutron detectors were used, n/ γ pulse shape discrimination, TOF (~ 50 cm). The neutron spectra measurements were done simultaneously for angles ranging from 0° to 180° in interval 18° relative to the light FFs direction.	$\leq 5\%$	---	0.04 ± 0.02
<i>Investigation of (n,n)-angular correlation</i>			
<u>C.B. Franklyn et.al. [26] (1978).</u> Two stilbene neutron detectors. The measurements were done for angles ranging from 9° to 180° in 9° interval between pairs of fission neutrons.	20%	---	Not investigated
<u>I.S. Guseva et.al. [27] (2018).</u> Two stilbene neutron detectors, n/ γ pulse shape discrimination.	$2.0 \pm 1.5\%$	1.8 ± 0.2 MeV	Weakly sensitive

Evaluations of the “scission” neutron yields [28-40] made in the framework of different theoretical models are in a quantitative agreement with the experimental evaluations given above. At the same time, there exists a sufficiently strong dependence of the obtained “scission” neutron yield on the parameters used for model calculations. Therefore, a final conclusion about validity of any mechanism of such neutron emission can be done only after detailed comparison of theoretical predictions with the dependences reliably observed in the experiment.

As is known, prompt fission γ -rays are emitted with a higher probability (~ 10 – 15%) along the direction of motion of fragments [41-44], which can indicate that fragments have a significant angular momentum ($\sim 7\hbar$) perpendicular to the direction of motion of fragments [41, 45]. In this case, such an effect can occur at the emission of PFNs from fragments [37, 46-49] and, therefore, a possible anisotropy of the angular distribution of PFNs in the center-of-mass system of fission fragments should be considered when analyzing data. However, as is seen in Fig. 1 (lower part), information on the anisotropy of the emission of PFNs in the center-of-mass system of fission fragments obtained from the analysis of measured angular and energy distributions of PFNs is even more scarce than information on the yield of “scission” neutrons.

A significant difference observed between the data of various experimental groups (Fig. 1 and Table 1) is related both with the uncertainties of the experimental data and the model calculations. The uncertainties of the parameters used in model calculations, such as the PFN spectrum, its dependence on the fission fragment characteristics, mass and kinetic energy distributions, are sufficiently large to explain, probably, a difference obtained in evaluations. In order to exclude these uncertainties, it is necessary to make a comparison of the PFN distributions obtained in the different experiments using the same models and parameters. However, such a comparison cannot be done because in the works mentioned above only the final conclusions are given without presentation of the actual experimental data. Presently, in the published experimental data base, there are limited data sets ($(^{252}\text{Cf}(\text{s.f}) - [8, 22, 50, 21], ^{235}\text{U}(\text{n}_{\text{th}},\text{f}) - [4, 25, 27], ^{233}\text{U}(\text{n}_{\text{th}},\text{f}) - [25, 27] \text{ и } ^{239}\text{Pu}(\text{n}_{\text{th}},\text{f}) - [27, 51])$), which can be used for independent evaluation in the framework of the considered the PFN emission model.

Among different experimental methods presently used for investigation of the PFN emission mechanism, the following ones can be highlighted: study of the angular and energy distributions of PFNs [1-8, 11-18, 20, 22-25]; study of the angular dependence of neutron – neutron coincidences in fission [9, 21, 26, 27, 52]; study of the E2-transitions for gamma-rays from fission fragments [53]; experiments on measuring a time of the coupled-neutron emission [54]; search for T-odd asymmetry in the PFN emission [55,56]. The most informative are the works on study of the angular and energy distributions of PFNs in laboratory system. Analysis of these distributions enables to obtain not only the yield of “scission” neutrons and their energy distribution, but also the anisotropy of neutron emission in the center-of-mass system of fission fragment, as well as to study the dependence of “scission” neutron yield on the fragment characteristics [11, 17, 23].

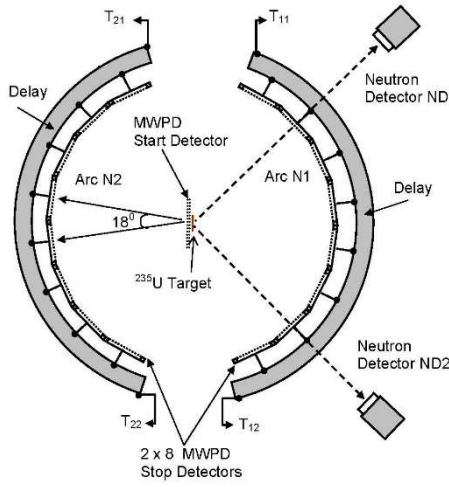
In 2008-2015, at the PNPI, a series of investigations was carried out using the same experimental set-up, intended to study the PFN angular and energy distributions in thermal-neutron induced fission $^{233}\text{U}(\text{n}_{\text{th}},\text{f})$, $^{235}\text{U}(\text{n}_{\text{th}},\text{f})$, $^{239}\text{Pu}(\text{n}_{\text{th}},\text{f})$ and spontaneous fission $^{252}\text{Cf}(\text{s.f})$. A special attention was paid not only to minimize possible systematic errors of measurements, but also to have a possibility to evaluate systematic errors. It was provided by means of symmetric geometry of the experiment which included 8 separate identical fragment detectors and 2 separate neutron detectors with similar parameters. The results of these investigations are given in publications [22, 25, 51, 56-58], while the numerical data obtained are presented in the EXFOR data base [59]. The preliminary data processing, procedures of the corrections calculation and implementation were analogous for all investigated nuclei.

In the present report are given the results of analysis of the PFN angular and energy distributions from thermal- neutron induced fission $^{233}\text{U}(\text{n}_{\text{th}},\text{f})$ and $^{235}\text{U}(\text{n}_{\text{th}},\text{f})$. In order to exclude uncertainties of the model calculations carried out using an assumption that all neutrons are emitted from the fully accelerated fragments, in the present work, in a course of the experimental data analysis it was used a method free of any assumptions about the PFN properties [25, 60].

1. Description of the experimental set-up

The experiments have been done at the radial neutron channel N7 of the research reactor WWR-M (PNPI, Gatchina) equipped with a neutron guide 3m in length. The detailed description of measurement technique and data processing has been given elsewhere [22, 60-62]. The spectra of PFNs were measured simultaneously for 11 angles between the direction of emission of a neutron and the direction of motion of a light fragment in the range of 0° – 180° with a step of 18° (Fig. 2). Taking into account the real geometry and angular resolution of experimental set-up, these angles were 8.8° , 19.9° , 36.8° , 54.5° , 72.2° , 90° , 107.8° , 125.5° , 143.2° , 160.1° , and 171.2° . The energies of PFNs and velocities of fission fragments were determined using the time-of-flight (TOF) technique.

The multi-wire proportional detectors (MWPD) were used to detect fission events and to determine directions of motion of fission fragments. The start MWPD located within a 7 mm range from the fissile target and parallel to the target plane was mounted together with the target holder-ring on a special frame located in the center of the reaction chamber filled with isobutene (~ 4 Torr) in such a way that all hardware parts were well out of the path of the neutron beam. The stop MWPDs were placed in the form of two arcs of eight detectors in the reaction chamber on a circle at a distance of 140 mm from the center of the chamber. The neutron beam was directed along the chamber axis.



The PFNs were detected by two neutron scintillation detectors (stilbene crystals $\varnothing 50$ mm \times h50 mm and $\varnothing 40$ mm \times h60 mm mounted on the Hamamatsu-R6091 phototubes) positioned with a 90° angle between their respective axes at a distance of about 50cm from the fissile target. Both neutron detectors were shielded by a cylindrical shield made of a 30mm thick layer of lead and a 40mm thick layer of polyethylene (not shown in Fig. 2). The neutron registration threshold was ~ 200 keV. A double-discrimination method (pulse shape and time-of-flight) was used to separate the events produced by neutrons and γ -quanta. The total time uncertainty of timing of signals of neutron detectors, which is determined as the FWHM of peak of γ -ray photon-fragment coincidences, was 1.0–1.2 ns.

Fig. 2. Experimental set-up

2. Model

2.1. General

In this work, the yield of “scission” neutrons is estimated by comparing the measured distributions of PFNs with model calculations under the assumption that all PFNs are emitted from fully accelerated fragments. Within this model, the spectrum of PFNs in the center-of-mass system of a fission fragment with known mass and kinetic energy completely determines the spectrum of PFNs in the laboratory system.

The number of neutrons $n_l(E, \theta)$ emitted with the energy E into unit solid angle at the angle θ with respect to the direction of fragment motion in the laboratory system is related to the number of neutrons $n_c(\varepsilon, \theta_c)$ emitted with the energy ε at the angle θ_c with respect to the direction of fragment motion in the center-of-mass system of the fragment as

$$n_l(E, \theta : m_f, TKE) = \sqrt{\frac{E}{\varepsilon}} \cdot (1 + A_2(\varepsilon) \cdot P_2(\cos \theta_c)) \cdot n_c(\varepsilon : m_f, TKE) \quad (1)$$

$$\varepsilon = E_f + E - 2 \cdot \cos(\theta) \cdot \sqrt{EE_f} \quad (2)$$

$$E_f = TKE \cdot \left(\frac{1}{m_f} - \frac{1}{A} \right) \quad (3)$$

$$\sqrt{\varepsilon} \cos(\theta_c) = \sqrt{E} \cdot \cos(\theta) - \sqrt{E_f} \quad (4)$$

$$n_{c,\theta}(\varepsilon : m_f, TKE) = \sqrt{\frac{\varepsilon}{E}} \cdot \frac{n_l(E, \theta : m_f, TKE)}{1 + A_2(\varepsilon) \cdot P_2(\cos \theta_c)} \quad (5)$$

$$N(E, \theta) = \sum_{m_f} \int_0^\infty \sqrt{\frac{E}{\varepsilon}} \cdot (1 + A_2(\varepsilon) \cdot P_2(\cos \theta_c)) \cdot n_c(\varepsilon : m_f, TKE) dTKE \quad (6)$$

Here, $N(E, \theta)$ is the integral number of neutron (without separation on certain mass split) with energy E observed in experiment and detected at angle θ relative to the fragment's direction, $n_c(\varepsilon)$ is the spectrum of PFNs in the center-of-mass system of the fission fragment (the case of isotropic distribution), $P_2(\cos \theta_c)$ is the second-order Legendre polynomial, $A_2(\varepsilon)$ is the anisotropy parameter of the angular distribution of PFNs in the center-of-mass system of the fission fragment due to a large angular momenta of the fragments ($\sim 7\hbar$ on average), as mentioned above, E_f is the energy per nucleon for a fragment with the mass m_f , A is the mass number of the fissioning nucleus, and TKE is the total kinetic energy of fission fragments.

According to the structure of Eqs. (1)–(4), the spectra of PFNs in the center-of-mass system of the fission fragment can be obtained from the spectra of the PFNs measured at different angles with respect to the direction of fragment motion (Eq. (5)). In this case, an individual spectrum of PFNs in the center-of-mass system of the fragment, $n_{c,\theta}(\varepsilon)$, is obtained for each given direction θ , and the test of the confidence of the model of emission of PFNs from fully accelerated fragments is reduced to the test of identity of the spectra $n_{c,\theta}(\varepsilon)$ within the reached accuracy of experimental data for different directions. In other words, the accuracy of the model is characterized by the deviation of the observed angular and energy distributions of PFNs in the laboratory system from the respective distributions calculated using Eq. (6) with $n_{c,\theta}(\varepsilon)$ as the spectrum of PFNs in the center-of-mass system of the fragment. The main advantage of this approach is that model distributions of PFNs that are necessary for comparison with experimental data can be determined without any assumptions on the character of distribution of neutrons between light and heavy fragments, on the form of the spectrum of PFNs in the center-of-mass system of the fragment, and on their dependence on the characteristics of fission fragments.

Strictly speaking, such a method of testing the model of emission of PFNs from fully accelerated fragments implies that the angular and energy distributions of PFNs are measured for various masses and kinetic energies of fragments. The accuracy of resulting estimates of the number of “scission” neutrons in this case is limited only by the experimentally reached resolution for the velocities of neutrons and fission fragments. Nevertheless, as was shown in [3-6, 24, 63], to construct model distributions of PFNs such as the angular and energy distributions $N(E, \theta)$ and total spectrum $\Phi(E)$, it is possible to use the approximation of two fragments according to which PFNs are emitted in the process of fission from two (light and heavy) fully accelerated fragments with fixed average masses and energies taken from literature (for instance, see Appendix 1-3).

In this approach the following equations are used:

$$\varepsilon = \bar{E}_{f,K} + E - 2 \cdot \cos(\theta) \cdot \sqrt{E \bar{E}_{f,K}} \quad (7)$$

$$\sqrt{\varepsilon} \cos(\theta_c) = \sqrt{E} \cdot \cos(\theta) - \sqrt{\bar{E}_{f,K}} \quad (8)$$

$$\bar{E}_{f,K} = \left\langle \frac{\nu_K(m_f, TKE) \cdot TKE}{\bar{\nu}_K} \cdot \left(\frac{1}{m_K} - \frac{1}{A} \right) \right\rangle \approx F_K \cdot \overline{TKE} \cdot \left(\frac{1}{m_K} - \frac{1}{A} \right) \quad (9)$$

Here, $K = L$ or H is the index indicating the light or heavy fragment, respectively; $\bar{E}_{f,K}$ is the average energy per nucleon for the light ($K = L$) or heavy ($K = H$) fragment; $F_K = 0.94$ – 0.97 is the coefficient reflecting the dependence of the yield of the PFNs on the characteristics of the fragment [64]; $\bar{\nu}_K$ is the average number of neutrons per fission event for the light or heavy fragment; $\nu_K(m_f, TKE)$ is the

average number of emitted neutrons as a function of the fragment characteristics; \overline{TKE} is the average total kinetic energy of fission fragments; \overline{m}_K is the average mass of the light or heavy fragment.

Then, the number of neutrons emitted from light or heavy fragments within unit energy interval per unit solid angle in the laboratory system, $n_{l,K}(E, \theta)$, is related to the analogous number of neutrons in the center-of-mass system of fission fragment, $n_{c,K}(\varepsilon, \theta_c)$, by means of the following formulas:

$$n_{l,K}(E, \theta) = \sqrt{\frac{E}{\varepsilon}} \cdot n_{c,K}(\varepsilon, \theta_c) = \sqrt{\frac{E}{\varepsilon}} \cdot n_{c,K}(\varepsilon) \cdot \varphi(\varepsilon, \theta_c) \quad (10)$$

$$\varphi(\varepsilon, \theta_c) = 1 + A_2 \cdot \varepsilon \cdot P_2(\cos \theta_c) \quad (11)$$

where function $\varphi(\varepsilon, \theta_c)$ is the angular distribution of neutrons in the center-of-mass system, A_2 is the anisotropy parameter of the angular distribution of PFNs in the center-of-mass system of the fission fragment.

The number of neutrons $n_l(E, \Omega)$ with energy E registered at angle Ω relative to the light fragment's direction in the laboratory system can be represented as the sum of contributions from the light $n_{l,L}(E, \Omega)$ and heavy fragments $n_{l,H}(E, \Omega)$:

$$n_l(E, \Omega) = n_{l,L}(E, \Omega) + n_{l,H}(E, \Omega), \quad (12)$$

$$n_{l,L}(E, \Omega) = n_{l,L}(E, \theta + \Delta_1) \quad \text{and} \quad n_{l,H}(E, \Omega) = n_{l,H}(E, 180 - \theta + \Delta_2),$$

where Δ_1 and Δ_2 are the terms due to the neutron recoil effect. In a case of thermal neutron induced fission, the deviations of fragment's directions of motion from co-linearity due to neutron recoil effect does not exceed 2° on average [65, 66], the terms Δ_1 and Δ_2 are usually taken equal to zero. In this work this correction were calculated (see Fig. 3) using the equation given in [66]. The integral spectrum $\Phi(E)$ of PFNs in the laboratory system is defined as follows:

$$\Phi(E) = 2\pi \cdot \int_0^\pi n(E, \Omega) \sin(\Omega) d\Omega \quad (13)$$

In this approximation it is also possible to obtain the spectra of PFNs in the center-of-mass system of the fission fragment by equation analogous to Eq. (5):

$$n_{c,K}^\theta(\varepsilon) = \sqrt{\frac{\varepsilon}{E}} \cdot \frac{n_{l,K}(E, \theta)}{1 + A_2(\varepsilon) \cdot P_2(\cos \theta_c)} \quad (14)$$

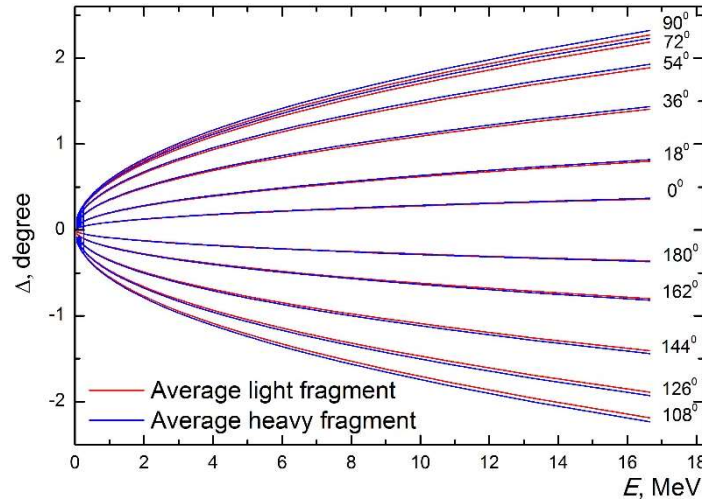


Fig. 3. Energy dependence of the correction due to neutron recoil for fixed angles θ given in the right part of the figure.

Further, by using these PFN spectra, the model angular and energy distributions of PFNs in the laboratory system can be calculated. The comparison between experimental data and model

distributions calculated under the assumption that all PFNs are emitted from fully accelerated fragments gives the possibility to estimate the yield and properties of “scission” neutrons.

For estimating the influence of two-fragment approximation on the obtained model distributions, we have compared the total PFN spectra of $^{252}\text{Cf}(s.f)$ calculated for all possible combinations of fragment masses and kinetic energies [17, 19] and the approximation of two (light and heavy) fragments with average parameters [22]. These spectra are presented in Fig. 4 in comparison with the standard PFN spectrum [67]. In order to demonstrate the difference more clearly, the PFN spectra were normalized to the Maxwell distribution ($T_M = 1.42$ MeV) as

$$\mu(E) = \frac{N_I(E)}{\bar{\nu}_p \cdot M(T_M, E)} = \frac{N_I(E) \cdot \sqrt{\pi \cdot T_M^3}}{\bar{\nu}_p \cdot 2 \cdot \sqrt{E} \cdot \exp(-E/T_M)} \quad (15)$$

where $M(T_M, E)$ is the Maxwell distribution, T_M is the temperature parameter (average energy of the Maxwell distribution $\langle E \rangle = 3T_M/2$).

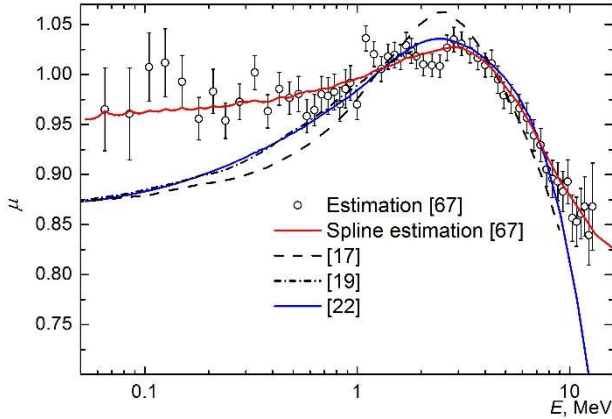


Fig. 4. Ratio of the total PFN spectrum of $^{252}\text{Cf}(sf)$ (normalized to average PFN number per fission) to the Maxwell distribution ($T_M = 1.42$ MeV): circles show estimated values from [67]; curves show the results of calculations for various combinations of fragment masses and kinetic energies [17, 19], and the approximation of two (light and heavy) fragments with average parameters [22].

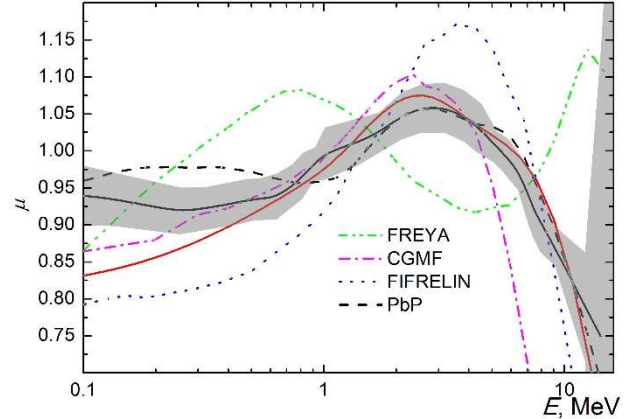


Fig. 5. (Color online) Ratio of the total PFN spectrum of $^{235}\text{U}(n_{th}, f)$ (normalized to average PFN number per fission) to the Maxwell distribution ($T_M = 1.32$ MeV): black curve corresponds to evaluated data (GMA-approximation [58], uncertainty is shaded by grey color); FREYA, CGMF, FIFRELIN, and PbP are models (program codes) from [58] used for calculation of PFN properties; red curve corresponds to the model calculations using two-fragment approximation.

As can be seen, the total spectra calculated for all possible combinations of fragment masses and kinetic energies using equations analogous to Eqs. (1)-(6) and (13) [17, 19] almost coincide with the approximation of two fragments with average parameters [22]. It was pointed out in [17, 22], as well as in [18] (the results of which were used in [19]), the best description of obtained data is achieved under assumption of the nonzero anisotropy of PFN emission in the center-of-mass system of fission fragment. The parameter of anisotropy A_2 estimated from the analysis of data amounted to 0.04 [17], 0.01 ± 0.02 [18], and 0.04 ± 0.02 [22]. In a more recent investigation [68] of the angular distribution of PFNs in the center-of-mass system of $^{252}\text{Cf}(sf)$ fission fragment, it was found that $A_2 = 0.020 \pm 0.003$. Analysis of the integral PFN spectrum of ^{252}Cf in the framework of modified Madland–Nix model [69] also showed the presence of anisotropy for PFN emission in the center-of-mass system of fission fragments.

It should be emphasized that the approach implemented in [17, 19, 22, 24] provides the best description of both partial and integral PFN distributions observed in the experiment. This result is not achieved with models (program codes) proposed for the numerical description of PFN characteristics [58]. Figure 5 presents the results of calculations performed using some of these codes for the total PFN spectrum of $^{235}\text{U}(n_{th}, f)$ with the same set of input parameters. As can be seen, the results are significantly different and only qualitatively consistent with the experiment. Nevertheless, the analysis of dependences obtained in the framework of various models (program codes) allows for some features of the fission

process to be elucidated, and gaps in the existing databases to be filled for fissioning nuclei and excitation energies for which experimental data are unavailable.

2.2. Analysis of PNPI's data

In present work, the estimation of yield of “scission” neutrons was performed using the data obtained at the PNPI. The spectra of PFNs in the center-of-mass system of fission fragment were obtained in the approximation of two fragments by Eqs. (7)–(14) using the spectra of neutrons $n_l(E, \Omega)$ measured for three selected detection angles relative to the fragment escape direction $\theta = 8.8^\circ, 19.9^\circ, 36.8^\circ$ ($\Omega < 40^\circ$), which correspond to $\Omega = 8.8^\circ, 19.9^\circ, 36.8^\circ$ for light fragments and to $\Omega = 171.2^\circ, 160.1^\circ, \text{ and } 143.2^\circ$ ($\Omega > 140^\circ$) for heavy fragments.

In this case, it is possible to obtain almost unlimited (in the low-energy range) PFN spectrum in the center-of-mass system of fission fragment and, hence, to minimize the uncertainty of model calculations related to uncertainty of the shape of spectra and the number of PFNs emitted from light and heavy fragments. In this approach, only two unknown parameters remain: average energies per nucleon for light and heavy fragments which are determined by Eq. (9). The obtained parameters are presented in Table 2. It should be noted that at the selected angles the contribution of neutrons from the complementary fragment to the measured neutron spectra is small and can be calculated with quite good accuracy [60, 64]. The procedure of determining and introducing this correction consists of the following steps.

Table 2. The input parameters of the model

	$^{233}\text{U}(\text{n},\text{f})$	$^{235}\text{U}(\text{n},\text{f})$	$^{239}\text{Pu}(\text{n},\text{f})$	$^{252}\text{Cf}(\text{sf})$
\overline{TKE} , MeV	170.5 ± 0.5	171.0 ± 0.6	177.5 ± 0.7	185.3 ± 0.9
\overline{m}_H	139.3 ± 0.2	139.7 ± 0.1	139.5 ± 0.1	143.5 ± 0.1
F_L	0.964 ± 0.005	0.962 ± 0.006	0.969 ± 0.005	0.975 ± 0.005
F_H	0.951 ± 0.007	0.950 ± 0.007	0.959 ± 0.005	0.971 ± 0.005
$\overline{E}_{f,L}$, MeV	1.033 ± 0.007	1.012 ± 0.007	0.995 ± 0.007	0.949 ± 0.007
$\overline{E}_{f,H}$, MeV	0.471 ± 0.004	0.474 ± 0.004	0.511 ± 0.004	0.540 ± 0.004

At the first step, it is assumed that neutrons detected for three selected angles relative to the light fragment's direction of motion in the laboratory system ($\Omega < 40^\circ$ for light fragments and $\Omega > 140^\circ$ for heavy fragments) are emitted from only the light and heavy fragments, respectively. Then, the neutron spectra measured for selected angles can be used for calculating neutron spectra in the center-of-mass system for the corresponding light and heavy fragments using Eq. (14). Only the events accumulated with $0 \leq \theta_c \leq 90^\circ$ are taken into account (in the center-of-mass system of fission fragment, the PFNs are emitted into the forward hemisphere with respect to the direction of motion of the fragment). These events were selected with the aid of relation

$$\sqrt{E} \cdot \cos(\theta) \geq \sqrt{\overline{E}_{f,K}} . \quad (16)$$

Then, the obtained neutron spectra in the center-of-mass system of fission fragment were used to determine the contribution of neutrons emitted from the complementary fragment. For example, Fig. 6 shows the angular distribution of the PFNs of $^{252}\text{Cf}(\text{s.f.})$ in the laboratory system and partial distributions for neutrons moving in direction of motion of the fragment and in the opposite direction taken from ref. [22]. It can be seen that the measured spectrum of PFNs always includes a fraction of neutrons from the complementary fragment, and the fraction of neutrons moving in the direction opposite to the direction of motion of fragments begins to dominate for angles larger than 50° . Consequently, before using the measured spectra of PFNs to determine the spectra of PFNs.

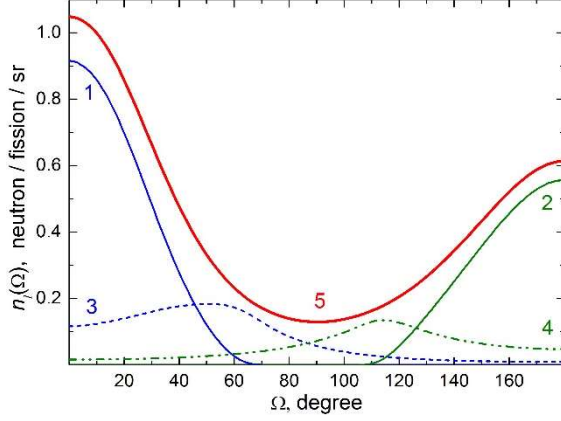


Fig. 6. Angular distributions of the PFNs from $^{252}\text{Cf}(sf)$ (in the laboratory system with respect to the direction of motion of the light fragment) that are emitted into the forward and backward hemispheres with respect to the plane perpendicular to the fission axis (lines 1, 2 and 3, 4 for the light and heavy fragments, respectively) obtained in model calculations for zero neutron detection threshold. Line 5 is the integral distribution.

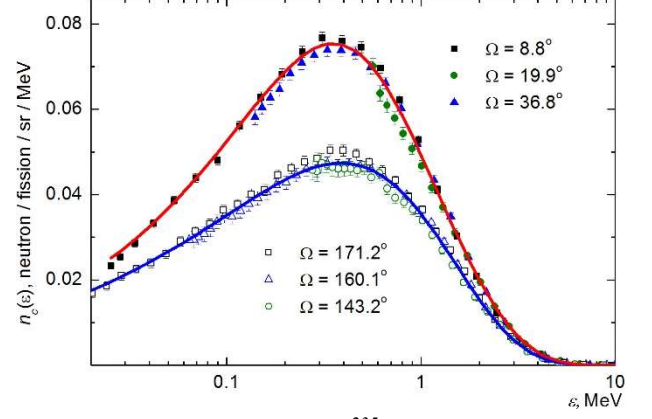


Fig. 7. The PFN spectra of $^{235}\text{U}(n, f)$ in the center-of-mass system of (black symbols) light and (open symbols) heavy fragments, obtained from spectra in the laboratory frame in the two-fragment approximation (in linear and logarithmic scales) for selected angles Ω between the neutron emission and light fragment escape directions; curves show the approximation according to formula (17).

in the center-of-mass system of the fission fragment, the contribution from the emission of PFN from the complementary fragment should be subtracted from them.

At the second step, the contribution of neutrons from the complementary fragment determined in the first step was subtracted from the spectra measured at angles $\Omega < 40^\circ$ (for light fragments) and $\Omega > 140^\circ$ (for heavy fragments) in the laboratory system. After that, the spectra of the PFNs in the center-of-mass system of the light and heavy fission fragments were recalculated and approximated by the following function with parameters $(\bar{\nu}_K, \omega_K, T_{1K}, T_{2K})$ determined by the least squares method:

$$n_{c,K}(\varepsilon) \cong \text{Fit}_K(\varepsilon) = \frac{\bar{\nu}_K}{4\pi} \cdot \left[\varpi_K \cdot \frac{\varepsilon}{T_{1K}^2} \cdot \exp\left(-\frac{\varepsilon}{T_{1K}}\right) + (1 - \varpi_K) \cdot \frac{2 \cdot \sqrt{\varepsilon}}{\sqrt{\pi} \cdot T_{2K}^3} \cdot \exp\left(-\frac{\varepsilon}{T_{2K}}\right) \right] \quad (17)$$

Here, $\bar{\nu}_K$ is the average number of neutrons per fission event for a light or heavy fragment ($\bar{\nu}_p = \bar{\nu}_L + \bar{\nu}_H$); ω_K is the weighing function; and T_{1K}, T_{2K} are the corresponding distribution parameters. For the convenient use and simplification of model calculations, function (17) was further used as the spectra of PFNs in the center-of-mass system of light and heavy fragments instead of discrete distributions obtained from experimental data. These basic spectra of neutrons in the center-of-mass system of fragments (for example, in fig. 7 the spectrum obtained for ^{235}U is presented) were used for calculating (with the help of expressions (7)–(13)) the angular and energy distributions of PFNs in the laboratory system, corresponding to the model of neutron emission from fully accelerated fission fragments.

3. Results

3.1. Comparison of the PNPI's experimental results and model calculation

Measurements were first made for thermal neutron induced fission ^{235}U [56, 60]. The difference between the measured PFN yield for angle $\Omega = 90^\circ$ and the neutron yield calculated using the model of neutron emission from fully accelerated fragments was found to be $\sim 10\%$ [60]. It was found that the description of the distributions can be improved by assuming that there is anisotropy of the angular distribution of PFNs in the center-of-mass system of fission fragment ($n_c(0^\circ)/n_c(90^\circ) \approx 1.08$). Under the assumption that the “scission” neutrons are emitted isotopically in the laboratory system, the fraction of these neutrons was estimated as $\sim 7\%$ of the total number of neutrons per fission event.

Further investigations with ^{252}Cf spontaneous fission and thermal neutron induced fission of ^{233}U showed that additional corrections should be introduced in the measured distributions, and the data processing procedure had to be changed [25, 62]. So, for determination of the PFN spectrum from the measured time-of-flight spectrum, a relativistic equation is used. Additionally, the following effects have been taken into account: neutron recoil, fragment transmission of the start and stop MWPDs, normalization correction connected to the fact that in the measurements we have the experimental histogram distributions instead of continuous distributions. Also, the angular and energy resolution corrections were applied by the approach more consistent than in Ref. [60]. The comparison of the results for thermal neutron induced fission of ^{235}U obtained before and after additional

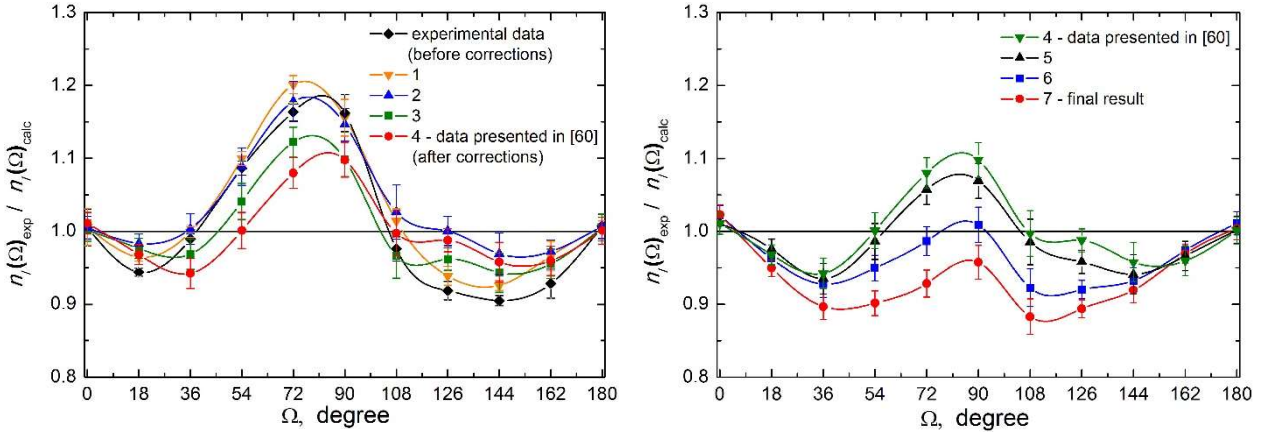


Fig. 8. Angular dependence of the ratio of measured neutron yield of ^{235}U and calculated one after corresponding corrections have been taken into account. Left part: the result presented in [60], the following corrections have been taken into account: 1- the correction for difference in solid angle and detector efficiency of fission fragments; 2 – the correction for complementary fragment contribution; 3 – the correction for angular resolution; 4 – neutron recoil correction were introduced into the model calculation. Right part: the same result obtained using additional corrections [62]: 5 - fragment transmission of the start and stop MWPDs; 6 – sum of several correction: normalization correction (connected to the fact that in the measurements the experimental histogram distributions were obtained instead of continuous distributions), correction for angular and energy resolutions of neutron detectors, for determination of prompt neutron energy spectrum from the measured time-of-flight spectrum, a relativistic equation is used; 7 – the real average angles instead of those with step 18° were introduced into the model calculation.

corrections were taken into account is presented in Fig. 8 along with the contribution of each of additional correction to the estimation of “scission” neutron derived. Additionally, the following feature was emphasized in Ref. [25]. The description of experimental data is improved if spectra measured for angles $\Omega < 40^\circ$ (light fragments) and $\Omega > 160^\circ$ (heavy fragments) are used as the basis spectra, rather than the spectra for small and large angles of 8.8° and 172.1° (as in Ref. [60]), respectively. This occurs because, first, the statistical accuracy of the initial spectra used to obtain the spectra in the center-of-mass system of the fragment, is improved. Second, the existing systematic error caused by uncertainty of the standard spectrum of PFNs from ^{252}Cf used in the correction for registration efficiency of neutron detectors and by the difference in the conditions of measurements of the spectra of PFNs for different angles, is partially compensated.

After the additional corrections have been introduced and model parameters have been optimized [25, 62], the PFNs yield from $^{233}\text{U}(n, f)$, $^{235}\text{U}(n, f)$, and $^{252}\text{Cf}(sf)$ at angles of $\sim 0^\circ$ and $\sim 90^\circ$ with respect to the direction of fragments could be described within the experimental errors by the model of isotropic neutron emission from fully accelerated fragments (Fig. 9, white symbols). The experimentally observed neutron deficits at angles close to $\sim 40^\circ$ and 140° , as compared to the model calculations, were adequately described by assuming that neutrons were emitted in the fission fragment center-of-mass system along the direction of motion of fission fragment with higher probability than perpendicular to this direction ($n_c(0^\circ)/n_c(90^\circ) \approx 1.07 \div 1.09$). It was also managed to describe not only the angular and energy distributions of the yield of PFNs but also their total spectrum in the laboratory system above 1 MeV and their average number per fission event (see Table 3).

The yield of “scission” neutrons in the ^{235}U fission, when they are isotopically distributed in the laboratory system, was estimated to be no greater than $\sim 3\%$. For ^{233}U the estimate was about 4%. Joint analysis of the measured angular and energy distributions of PFNs in the ^{235}U and ^{233}U fission for fixed fission fragments showed that the measured dependence of the neutron yield on the mass and total kinetic energy of the fragments agreed with the literature data (Fig. 10). No appreciable dependence of the yield of “scission” neutrons on the characteristics of the fragments was found [25]. The dependence of the model calculation on the input parameters was investigated.

Table 3. Average total number of PFNs per fission event.

Target	v_{prompt} (neutron / fission)			
	Model calculation		Experiment	Evaluated data [58]
	$A_2 = 0$	$A_2 = 0.04$		
$^{252}\text{Cf}(sf)$	3.86	3.73	3.77 ± 0.03	3.7610 ± 0.0051
$^{235}\text{U}(n_{th}, f)$	2.56	2.45	2.44 ± 0.05	2.4184 ± 0.0021
$^{233}\text{U}(n_{th}, f)$	2.60	2.48	2.54 ± 0.06	2.4904 ± 0.0040

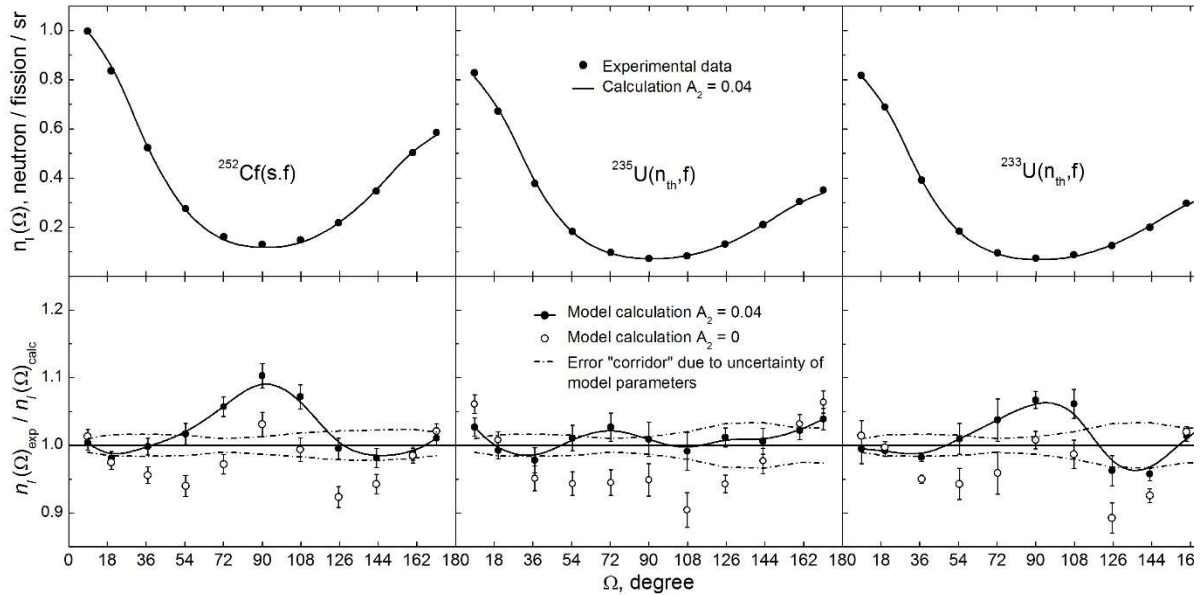


Fig. 9. Comparison of measurements and model calculations. Upper part: measured dependence of the PFN yield on the angle between the neutron and light fragment directions in the laboratory system; the curve is the calculation under the assumption that the angular distribution of neutrons in the fragment’s center-of-mass system is anisotropic ($n_c(0^\circ)/n_c(90^\circ) \approx 1.07 \div 1.09$). Lower part: (○) ratio of the measured PFN yield to the neutron yield calculated for isotropic neutron emission in the fragment’s center-of-mass system and (●) assuming anisotropic neutron emission ($n_c(0^\circ)/n_c(90^\circ) \approx 1.07 \div 1.09$). The interval of the errors due to uncertainty of the PFN spectra in the fragment center-of-mass system is limited by dotted and dashed curves.

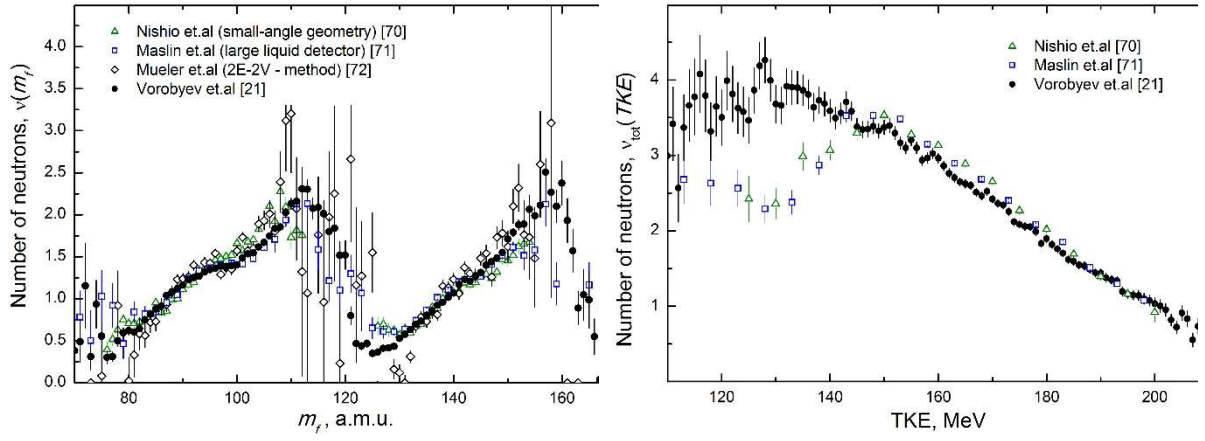


Fig. 10. The neutron yield as a function of pre-neutron fragment mass (left part) and TKE (right part) together with pre-neutron fission fragment mass and TKE distribution (for $^{235}\text{U}(n_{th}, f)$) [25].

It was demonstrated that the yields of PFNs at angles of $\sim 0^\circ$ and $\sim 90^\circ$ in the ^{235}U fission obtained by model calculations using all possible mass and kinetic energy combinations of fragments, and by the calculations in the approximation of two fragments with average parameters almost coincide. In the mentioned work [25] it was also estimated the sensitivity of the model (two-fragment approximation) to average parameters of fission fragments used in calculation. It was found that variation of these parameters within the accuracy assigned to the literature data (for example, in ^{235}U case, the value of energies per nucleon is 0.47-0.49 MeV for the heavy fragments and 1.01-1.04 MeV for light fragments) results in up to 4% variation in the calculated PFN yield for angles close to 90° , which corresponds to the “scission” neutron yield of $\sim 2\%$ per fission event.

The measurements of the total PFN spectra of ^{233}U and ^{235}U were carried out later [62, 73] in PNPI at the same experimental set-up. Figs. 11, 12 show the total PFN spectra $\Phi(E)$ of $^{235}\text{U}(n_{th}, f)$ and $^{233}\text{U}(n_{th}, f)$ obtained and normalized to Maxwell distribution with the temperature parameter $T_M = 1.32$ MeV Eq. (15). A comparison of these total PFN spectra to the estimated spectra (GMA least squares approximation [58] performed using published experimental data) shows a coincidence within experimental accuracy. This agreement is an evidence of the absence of any significant systematic errors in the angular and energy distributions of PFNs obtained in the PNPI.

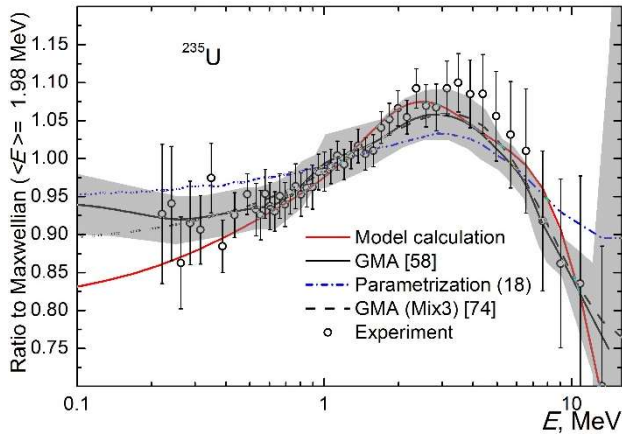


Fig. 11. Ratio of the total PFN spectrum of $^{235}\text{U}(n_{th}, f)$ (normalized to average PFN number per fission) to Maxwell distribution ($T_M = 1.32$ MeV): circles present data of measurements [62]; (black solid curve) estimated data (GMA [58]) with uncertainty area indicated by gray shade; (dash-dot curve) parameterization according to (18); (dash curve) estimated data (GMA (Mix 3) [74]); (bottom [red] curve) two fragment approximation with anisotropy parameter $A_2 = 0.04$.

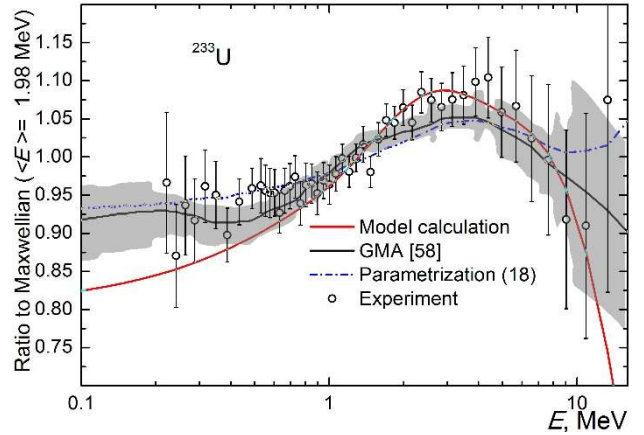


Fig. 12. Ratio of the total PFN spectrum of $^{233}\text{U}(n_{th}, f)$ (normalized to average PFN number per fission) to Maxwell distribution ($T_M = 1.32$ MeV): circles present data of measurements [73]; (black solid curve) estimated data (GMA [58]) with uncertainty area indicated by gray shade; (dash-dot curve) parameterization according to (18); (bottom [red] curve) two fragment approximation with anisotropy parameter $A_2 = 0.04$.

Note that the conclusion about the discrepancies between measured and model yields of PFNs, in a systematic sense, is weakly dependent ($\sim 3\text{-}5\%$ in equatorial emission) on the choice of the standard neutron spectrum used for efficiency correction of neutron detectors. In order to exclude the influence of the shape of total PFN energy spectrum on the estimated yield of “scission” neutrons, the measured angular and energy distributions have been newly corrected for neutron detector efficiency. This correction factor was defined as the ratio of total PFN spectra of $^{235}\text{U}(n_{\text{th}}, f)$ and $^{233}\text{U}(n_{\text{th}}, f)$ [62, 73] to the corresponding known total PFN spectra, respectively. In the present work, these reference spectra were obtained using the experimental fact [75] that the ratio of total spectra for X fissile nucleus and $^{252}\text{Cf}(s.f)$ can be described with sufficient accuracy as the ratio of two Maxwell distributions $M(T_M, E)$ with the corresponding parameters T_M :

$$\left(\frac{\Phi(E)}{\bar{\nu}_p} \right)_X \bigg/ \left(\frac{\Phi(E)}{\bar{\nu}_p} \right)_{\text{Cf}} = \frac{M_X(T_M, E)}{M_{\text{Cf}}(1.42, E)} \quad (18)$$

Since the Maxwell distribution parameter $T_M = 1.42$ MeV was established [67] to provide for the best description of experimental total PFN spectrum of ^{252}Cf and the final average energies derived from GMA approximation [58] are 2.000 ± 0.010 MeV ($T_M = 1.33$ MeV) for ^{235}U and 2.030 ± 0.013 MeV ($T_M = 1.35$ MeV) for ^{233}U , these parameters were used for obtaining additional corrections. The spline approximation $\Phi(E)$ of the estimated ^{252}Cf fission spectrum reported in [67] was adopted as reference total spectrum of PFNs from ^{252}Cf spontaneous fission for Eq. (18). It is convenient because it enables to make a recalculation later while the numerical data on the evaluated spectra are absent. The reference total PFN spectra of $^{235}\text{U}(n_{\text{th}}, f)$ and $^{233}\text{U}(n_{\text{th}}, f)$ fission calculated using Eq. (18) are presented in Figs. 11 and 12 together with the results of estimation (GMA approximation [58]) obtained from published experimental data by generalized least squares method. As can be seen, the relation (18) and model independent estimation based on GMA approximation [58] can be used for determining additional corrections.

In this work the preliminary processing and the determination and introduction of corrections were done in a similar way for $^{235}\text{U}(n_{\text{th}}, f)$, $^{233}\text{U}(n_{\text{th}}, f)$ and $^{252}\text{Cf}(s.f)$. The efficiency of the neutron detectors was determined as the ratio between the total PFN spectrum obtained by summing the measured neutron distributions over the angle of the measured distributions of neutrons and the reference spectrum obtained by means of Eq. (18). The parameters of the model used to calculate the angular and energy distributions of PFNs by assuming that they were emitted from the fully accelerated fragments were optimized to produce the best description of all data obtained in PNPI [58].

The total PFN spectra of $^{233}\text{U}(n_{\text{th}}, f)$ and $^{235}\text{U}(n_{\text{th}}, f)$ fission, as well as the total PFN spectrum of $^{252}\text{Cf}(sf)$, are presented in Figs. 11, 12 and 4 reveal some differences between the shape of experimental (estimated) PFN spectra and that of the spectrum calculated using the scheme described above (for two-fragment approximation) in the range of PFN energies below 0.6 MeV. These differences can be related to the following circumstances: (i) existence of “scission” neutrons; (ii) calculation errors; (iii) limitations of computational scheme; and (iv) implicit systematic errors in experimental (estimated) PFN spectrum, which can be due to both the errors of available experimental data and the method of their description. Significant computational errors can be excluded, since the results of calculations (Fig. 4) based on the data of various (methodologically different) methods [17, 19, 22] almost coincide. Herewith the total PFN spectra calculated using the scheme of two fragment approximation described above almost perfectly coincide with the spectra obtained in the framework of Madland–Nix model (ENDF/B-VII) adapted for best description of the available experimental data [58]. Restricted character of the aforementioned scheme of calculations is only determined by the accuracy of the measured angular distributions of PFNs. Therefore, the observed deviation can be treated as evidence of the existence of “scission” neutrons and, hence, their yield can be determined from the difference between experimental and calculated total spectra.

The main advantage of this approach to estimation of the yield of “scission” neutrons is that it depends only on two parameters: the shape of total PFN spectrum in the laboratory system and the total number of PFNs per fission event. Estimations of these factors, obtained by experts for nuclei widely encountered in practice, can be used for the comparative analysis. It is necessary to take into account that any systematic errors of the total PFN spectrum related to the quality of experimental data used for this estimation and the method of obtaining this estimate can lead to different conclusions concerning not only the yield of “scission” neutrons, but their existence as such.

From this standpoint, in making the aforementioned comparison, one should prefer estimating the total PFN spectrum in a model-independent form. To increase the reliability of determination of the yield of “scission” neutrons, it is necessary to confirm in the range of neutron energies below 0.6 MeV the presence of deviation of the experimentally measured/estimated PFN spectrum from that calculated assuming the PFM emission by fully accelerated fragments. For this purpose, it is necessary to carry out additional experimental investigations with participation of independent research groups using different neutron and fission fragment detectors for a number of various fissile nuclei, so as to exclude systematic errors inherent in any experimental investigation method. This is a task for the nearest future, requiring properly coordinated work of many experimenters.

A qualitative step toward solving questions concerning the existence of “scission” neutrons and their formation mechanisms can be based on studying the angular and energy distributions of PFNs. It was found that for neutron detection angles $\Omega = 90^\circ$, a neutron excess is observed relative to the model calculations: $4.6 \pm 2.7\%$, $5.9 \pm 2.8\%$, and $7.6 \pm 2.8\%$ for ^{233}U , ^{235}U , and ^{252}Cf , respectively. As mentioned above, the excess of the neutron yield relative to calculated values is also observed in the total PFN spectra in the region of neutron energies below 0.6–1 MeV (see Figs. 11, 12 and 4). Then, the yield of “scission” neutrons and their spectrum can be determined. As an example, Fig. 13 shows the angular dependence of the yield of “scission” neutron from $^{235}\text{U}(n, f)$ fission calculated by Carjan et.al. [34, 35] in a framework of a dynamical scission model under different initial condition and that obtained in this work as the difference between yields of PFNs measured and one calculated in the assumption that all PFNs was emitted from fully accelerated fragments. The qualitative agreement can be seen which leads to the conclusion that the PFN angular and energy distributions can be described using an assumption that the observed neutron

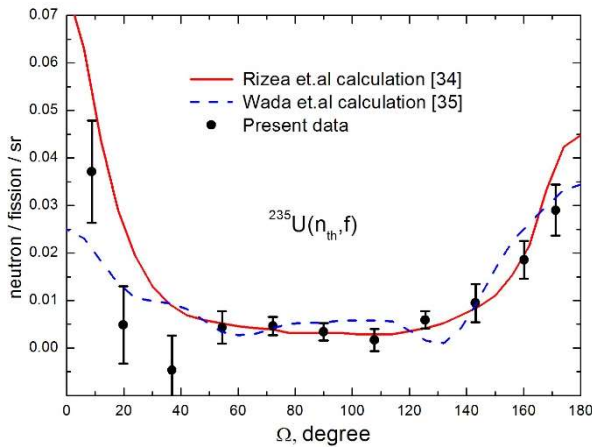


Fig.13. Angular dependence of the yield of “scission” neutrons from $^{235}\text{U}(n, f)$ fission: (●) the difference between the measured and model neutron yields for the angles Ω , the indicated errors include statistical errors and the uncertainty of model parameters. Straight curve – Rizea et.al calculation [34] performed on the surface of a sphere of radius $R=30$ fm and for time T further away from the moment of scission is $2 \cdot 10^{-21}$ sec. Dash line Wada et.al calculation [35] – $R=50$ fm, $T = 4 \cdot 10^{-21}$ sec and the effects of the scattering and re-absorption by the fission fragments on the angular distribution of scission particles were included into calculation.

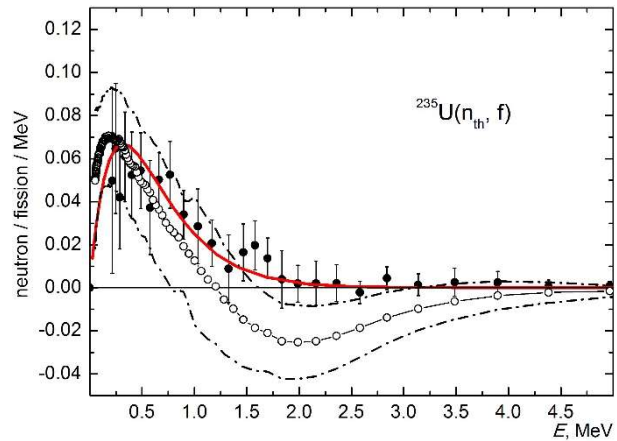


Fig. 14. Spectrum of “scission” neutrons from the $^{235}\text{U}(n, f)$ fission: (●) the difference between the measured and model neutron spectra for the angles Ω close to 90° ($\Omega = 72.2^\circ, 90^\circ, 108.8^\circ$) multiplied by 4π (first approach), the indicated errors are statistical; (—○—) the difference between the reference total PFN spectrum obtained by means of Eq. (18) and the model calculated total PFN spectrum (second approach). The interval of errors arising from uncertainty of the reference PFN spectrum is limited by the dotted-and-dashed lines. The curve is the approximation by function (19).

excess is associated with the dynamical effects analogous to those proposed in [34, 35].

In Fig.14 it is presented the spectrum of ^{235}U “scission” neutrons obtained in two different ways. In the first, the desired spectrum was defined as the difference between the measured and model neutron spectra for angles Ω close to 90° ($\Omega = 72.2^\circ, 90^\circ$ и 108.8°). In the second, the total spectrum of “scission” neutrons was defined as the difference between the reference total PFNs spectrum and model calculation.

To compare the two estimates, the “scission” neutron spectrum obtained in the first way was multiplied by 4π (it was assumed that the distribution of “scission” neutrons in the laboratory system was isotropic). A comparison of the spectra obtained in this manner shows the agreement (within the errors of the experimental data) between the results from estimates performed in different ways.

Since the relative contribution from “scission” neutrons should be largest at angles Ω close to 90° , the yield of these neutrons from the fission of the investigated nuclei was estimated using the spectrum obtained in the first way: with least squares approximated by functions (19) and (20):

$$p_s(E) = p_0 \cdot \frac{E}{T_0^2} \cdot \exp\left(-\frac{E}{T_0}\right), \quad (19)$$

$$p_s(E) = p_0 \cdot \frac{E}{T_0^2} \cdot \exp\left(-\frac{E}{T_0}\right) + p_1 \cdot \frac{E}{T_1^2} \cdot \exp\left(-\frac{E}{T_1}\right). \quad (20)$$

All parameters p_0 , T_0 , p_1 , T_1 were varied. The results of these approximations are given in Table 4.

Table 4. Main characteristics of “scission” neutrons.

	$^{233}\text{U}(\text{n,f})$	$^{235}\text{U}(\text{n,f})$	$^{252}\text{Cf}(\text{sf})$
Approximation using function (19)			
Yield, %	1.5 ± 0.6	1.8 ± 0.6	2.0 ± 0.6
Average energy, MeV	0.53 ± 0.08	0.47 ± 0.05	0.58 ± 0.06
Approximation using function (20)			
Yield, %	2.7 ± 0.8	2.6 ± 0.8	3.0 ± 0.8
Average energy, MeV	1.7 ± 0.2	1.4 ± 0.2	1.5 ± 0.2

Up to now the “scission” neutron spectrum were only calculated for ^{252}Cf [31]. In this calculation it is taking into account nonadiabatic effects in the interaction of the single-particle degrees of freedom with fragment acceleration. The obtained difference spectrum (“scission” neutron spectrum) for spontaneous ^{252}Cf fission can be qualitatively compared to this calculation. It is seen that the spectrum of “scission” neutrons [31] can be adequately described as well as angular dependence of their yield [34, 35] by assuming that the neutron excess observed in the experiment was due to the dynamic effects in nuclear fission.

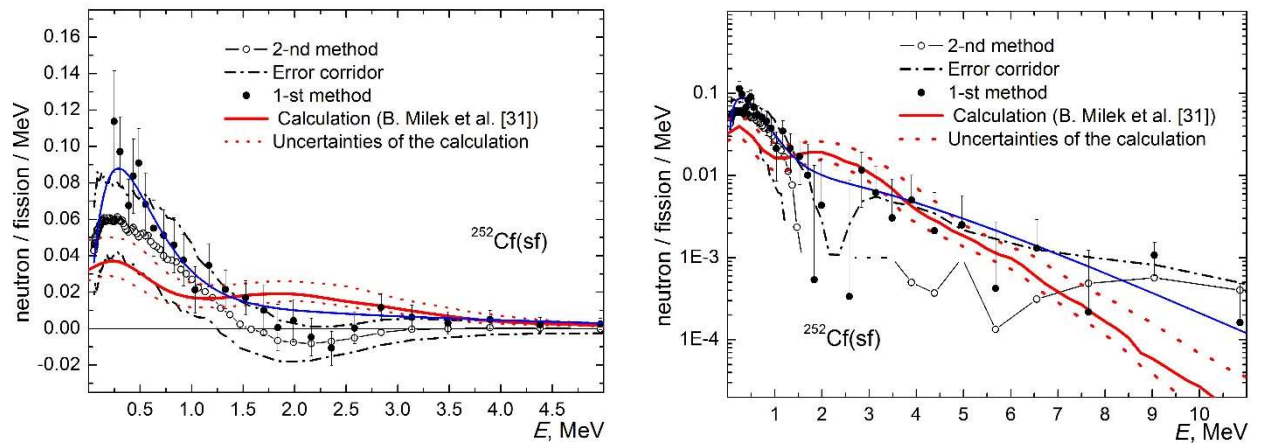


Fig. 15. Spectrum of “scission” neutrons from the $^{252}\text{Cf}(\text{sf})$ fission. Denotations are the same as in Fig. 8. The curve is the result of approximation using function (20). The dashed line is the scission neutron yield calculated in [31]. The dotted line shows the errors of calculation [31] arising from uncertainty of the input parameters; (a) and (b) are the linear and logarithmic scales respectively.

Conclusion

A comparison of the measured data and our model calculations shows that the experimentally observed average total number of neutrons per fission event, the total PFN spectrum, the dependence of the PFN yield on the characteristics of the fragments, and the angular and energy distributions of PFNs are described within the model of isotropic neutron emission from fully accelerated fragments with an error less than 10%.

Detailed analysis of the data shows that the model calculations must be performed using the anisotropy of prompt neutron emission in the center-of-mass system of fission fragment. It was found that in the center-of-mass system of fission fragment, the PFNs are emitted along the fission axis with a higher probability than perpendicular to it ($n_c(0^\circ)/n_c(90^\circ) \approx 1.07\text{--}1.09$).

The total spectrum of PFNs was calculated for investigated nuclei by assuming that the neutron emission from fully accelerated fragments coincides with the measured spectra within the errors of the experimental data in the neutron energy region of 0.6 to 10 MeV, and the average total number of neutrons per fission event is close to the recommended values. In the region of neutron energies below $\sim 0.6\text{--}1$ MeV, a neutron excess was observed in the experiment, relative to the model calculations.

The angular and energy distributions of PFNs in the laboratory coordinate system agree with the model calculations for all angles except those close to 90° with respect to the direction of fragments. An excess of neutrons observed at angle $\Omega = 90^\circ$ over the model calculations performed assuming that all PFNs are emitted from fully accelerated fragments reaches $4.6 \pm 2.7\%$ and $5.9 \pm 2.8\%$ for ^{233}U and ^{235}U , respectively.

The observed neutron excess cannot be explained within the model of neutron emission from fully accelerated fragments. This difference can be eliminated by assuming that there were $\sim 2\text{--}4\%$ of “scission” neutrons. The nature of the observed neutron excess can be determined after a thorough comparison of the experimental data and the calculations using theoretical models that allow for possible PFN emission mechanisms in fission.

References

1. R.R. Wilson, Phys. Rev. **72**, 189 (1947).
2. J.S. Fraser, Phys. Rev. **88**, 536 (1952).
3. J. Terrell, Phys. Rev. **113**, 527 (1959).
4. K. Skarsvag and K. Bergheim, Nucl. Phys. **45**, 72 (1963).
5. S.R. Ramanna, R. Chaudhry, S.S. Kapoor, K. Mikke, S.R.S. Murthy, P.N. Rama Rao, Nucl. Phys. **25**, 136 (1961).
6. S.S. Kapoor, R. Ramanna, and P.N. Rama Rao, Phys. Rev. **131**, 283 (1963).
7. J.S. Fraser and J.C. Milton, Annu. Rev. Nucl. Sci. **16**, 379 (1966).
8. H.R. Bowman, S.G. Thompson, J.C.D. Milton, and W.J. Swiatecki, Phys. Rev. **126**, 2120 (1962).
9. J.S. Pringle and F.D. Brooks, Phys. Rev. Letters, **35**, 1563 (1975).
10. Z. Fraenkel, I. Mayk, J.P. Unik, A.J. Gorski, and W.D. Loveland, Phys. Rev. **C 12**, 1809 (1975).
11. V. M. Piksaikin, P. P. D'yachenko, and L. S. Kutsaeva, Sov. J. Nucl. Phys. **25**, 385 (1977).
12. Yu. S. Zamyatnin, D. K. Ryazanov, B. G. Basova, et al., Sov. J. Nucl. Phys. **29**, 306 (1979).
13. P. Riehs, Acta Physica Austriaca **53**, 271 (1981).
14. D. Ward, R.J. Charity, D.J. Hinde, J.R. Leigh, and J.O. Newton, Nucl. Phys. **A403**, 189 (1983).
15. E.A. Seregina, P.P. Dyachenko, Yad. Fiz. **42**, 1337 (1985) (in Russian).
16. H. Marten, Proc. of IAEA Consulting Meeting, INDC(NDS)-251 (Vienna, 1991), p. 23.
17. O.I. Batenkov, A.B. Blinov, M.V. Blinov, S.N. Smirnov, Proc. of IAEA Consulting Meeting, INDC(NDS)-220, Vienna (1989), p.207.
18. C. Budtz-Jorgensen and H.-H. Knitter, Nucl. Phys. A **490**, 307 (1988).
19. U. Brosa and H.H. Knitter, Z. Phys. **A343**, 39 (1992).
20. Yu. D. Kamarzhnov, V. G. Nedopekin, V. I. Rogov, and S. T. Sukhorukov, At. Energy **84**, 393 (1998).
21. V.E. Sokolov, G.A. Petrov, I.S. Guseva, G.V. Val'sky, A.M. Gagarski, D.V. Nikolaev, D.O. Krinitsin, V.I. Petrova, T.A. Zavarukhina, Proc. of the XVIII-th International Seminar on Interaction

- of Neutrons with Nuclei “Neutron Spectroscopy, Nuclear Structure, Related Topics”, ISINN-18, Dubna, May 26-29, 2010, ed. A.M. Sukhovoij, JINR, Dubna, E3-2011-26 (2011), p. 108.
22. A.S. Vorobyev, O.A. Shcherbakov, A.M. Gagariski, G.A. Petrov, G. V. Val’ski, Journal of Experimental and Theoretical Physics **125**(4), 619 (2017).
 23. M.S. Samant, R.P. Anand, R.K. Choudhury, S.S. Kapoor, D.M. Nadkarni, Phys. Rev. C, **51** (1995) 3127.
 24. N.V. Kornilov, A.B. Kagalenko and F.-J. Hambsch, Phys. At. Nucl. **64**(8), 1373 (2001).
 25. A.S. Vorobyev, O.A. Shcherbakov, A.M. Gagariski, G.V. Val’ski, G.A. Petrov, EPJ Web of Conf. **8** (2010) 03004.
 26. C.B. Franklyn, C. Hofmeyer and D.W. Mingay, Phys. Lett. **78B**, 564 (1978).
 27. I.S. Guseva, A.M. Gagariski, V.E. Sokolov, G.A. Petrov, A.S. Vorobyev, G.V. Val’skiy, T.A. Zavarukhina, Physics of Atomic Nuclei **81**(4), 447 (2018).
 28. P. Madler, Z. Phys. A **321**, 343 (1985).
 29. R. W. Fuller, Phys. Rev. **126**, 684 (1962).
 30. Y. Boneh, Z. Fraenkel, Phys. Rev. C **10**, 893 (1974).
 31. B. Milek, R. Reif, and J. Revai, Phys. Rev. C **37**, 1077 (1988).
 32. H. Marten and D. Seeliger, J. Phys. G: Nucl. Phys. **14**, 211 (1988).
 33. N. Carjan, P. Talou, and O. Serot, Nucl. Phys. A **792**, 102 (2007).
 34. M. Rizea, N. Carjan, and T. Wada, Physics Procedia **47**, 27 (2013).
 35. T. Wada, T. Asano, and N. Carjan, Physics Procedia **64**, 34 (2015).
 36. V. P. Eismont, Sov. At. Energy **19**, 1000 (1965).
 37. K. Skarsvag, Physica Scripta **7**, 160 (1973).
 38. D.J. Hinde, R.J. Charity, G.S. Foote, J.R. Leigh, J.O. Newton, S. Ogaza, and A. Chattefjee, Phys. Rev. Letters **52**(12), 986 (1984).
 39. A. Matsumoto, H. Taninaka, K. Hashimoto, and T. Ohsawa, J. Nucl. Sci. Tech. **49**, 782 (2012).
 40. G. V. Val’skiy, Phys. At. Nucl. **67**, 1264 (2004).
 41. M.M. Hoffman, Phys. Rev. **133**, B714 (1964).
 42. G.A. Petrov, Sov. J. Nucl. Phys. **1**, 338 (1965).
 43. K. Skarsvag, Phys. Rev. C **22**, 638 (1980).
 44. G.V. Valsky, A.M. Gagariski, I.S. Guseva, D.O. Krinitsin, G.A. Petrov, Yu.S. Pleva, V.E. Sokolov, V.I. Petrova, T.A. Zavarukhina, and T.E. Kuzmina, Bulletin of the Russian Academy of Science: Physics **74**(6), 767 (2010).
 45. J.B. Wilhelmy, E. Cheifetz, R.C. Jared, S.G. Thompson, and H.R. Bowman, Phys. Rev. C **5**, 2041 (1972).
 46. T. Ericson and V.M. Strutinski, Nucl. Phys. **8**, 284 (1958).
 47. A. Gavron, Phys. Rev. C **13**, 2562 (1976).
 48. V. E. Bunakov, I. S. Guseva, S. G. Kadenskii, and G. A. Petrov, Izv. Akad. Nauk, Ser. Fiz. **70**, 1618 (2006).
 49. J. Randrup, R. Vogt, Physics Procedia **64**, 19 (2015).
 50. E. A. Seregina, P. P. D’yachenko, Vopr. At. Nauki Tekh., Ser.: Yad. Konstanty, No. **1**, 58 (1985).
 51. A.S. Vorobyev, O.A. Shcherbakov, A.M. Gagariski, G.A. Petrov, G.V. Val’ski, T.E. Kuz’mina, Journal of Experimental and Theoretical Physics **127**(4), 659 (2018).
 52. Yu. Kopatch, A. Chietera, L. Stuttge, F. Gonnenwein, M. Mutterer, A. Gagariski, I. Guseva, E. Chernysheva, O. Dorvaux, F.-J. Hambsch, F. Hanappe, Z. Mezentseva, S. Telezhnikov, Physics Procedia **64**, 171 (2015).
 53. L.K. Hwang, A.V. Ramayya, J.H. Hamilton, W. Greiner, J.D. Core, G.M. Ter-Akopian, Yu.Ts. Oganessian, A.V. Daniel, Phys. Rev. C, **60**, 044616 (1999).
 54. Yu.D. Katarzhnov, V.G. Nedopekin, V.I. Rogov, and S.T. Sukhorukov, Physics of Atomic Nuclei, **64**(2), (2001) 177.
 55. G.V. Danilyan, J. Klenke, V.A. Krakhotin, Yu.N. Kopach, V.V. Novitsky, V.S. Pavlov, P.B. Shatalov, Physics of Atomic Nuclei, **74**(5), 671 (2011).
 56. G.A. Petrov, A.M. Gagariski, I.S. Guseva, V.E. Sokolov, G.V. Val’ski, A.S. Vorobiev, D.O. Krinitsin, O.A. Shcherbakov, D.V. Nikolaev, Yu.S. Pleva, V.I. Petrova, T.A. Zavarukhina, Phys. At. Nucl. **71**, 1137 (2008).
 57. A.S. Vorobyev, G.V. Val’ski, A.M. Gagariski, I.S. Guseva, G.A. Petrov, V.I. Petrova, A.Yu. Serebrin, V.E. Sokolov, O.A. Shcherbakov, Crystallography Reports **56**(7), 1253 (2011).

58. R. Capote, Y.-J. Chen, F.-J. Hamsch, N.V. Kornilov, J.P. Lestone, O. Litaize, B. Morillon, D. Neudecker, S. Oberstedt, T. Ohsawa, N. Otuka, V.G. Pronyaev, A. Saxena, O. Serot, O.A. Shcherbakov, N.-C. Shu, D.L. Smith, P. Talou, A. Trkov, A.C. Tudora, R. Vogt, A.S. Vorobyev, *Nuclear Data Sheets* **131**, 1 (2016).
59. N. Otuka, E. Dupont, V. Semkova, B. Pritychenko, A.I. Blokhin, et al., *Nuclear Data Sheets* **120**, 272 (2014).
60. A.S. Vorobyev, O.A. Shcherbakov, Yu.S. Pleva, A.M. GagarSKI, G.V. Val'ski, G.A. Petrov, V.I. Petrova, and T.A. Zavarukhina, *Nucl. Instr. and Meth. in Phys. Res. A* **598**, 795 (2009).
61. A.S. Vorobyev, O.A. Shcherbakov, Yu.S. Pleva, A.M. GagarSKI, G.V. Val'ski, G.A. Petrov, V.I. Petrova, T.A. Zavarukhina, *Proc. of the XVII-th International Seminar on Interaction of Neutrons with Nuclei "Neutron Spectroscopy, Nuclear Structure, Related Topics", ISINN-17, Dubna, May 27-29, 2009*, ed. A.M. Sukhovej, JINR, Dubna, E3-2010-36, 2010, p. 60.
62. A. S. Vorobyev and O. A. Shcherbakov, *Vopr. At. Nauki Tekh., Ser.: Yad. Konstanty*, Nos. 1–2, 37 (2011–2012).
63. D.G. Madland and J.R. Nix, *Nucl. Sci. Eng.* **81**, 213 (1982).
64. J. Terrell, *Phys. Rev.* **127**, 880 (1962).
65. J. C. D. Milton and J. S. Fraser, *Phys. Rev.* **111**, 877 (1958).
66. T. Haninger, F.-J. Hartmann, P. Hofmann, Y. S. Kim, M. S. Lotfranaei, T. von Egidy, H. Marten, and A. Ruben, *Nucl. Phys. A* **572**, 294 (1994).
67. W. Mannhart, *Proc. of IAEA Consulting Meeting, INDC(NDS)-220, Vienna* (1989), p. 305.
68. A. Göök, F.-J. Hamsch, and M. Vadali, *Phys. Rev. C* **90**, 064611 (2014).
69. A. D. G. Madland and A. C. Kahler, *Nucl. Phys. A* **957**, 289 (2017).
70. K. Nishio, Y. Nakagome, H. Yamamoto, I. Kimura, *Nucl. Phys. A* **632**, 540 (1998).
71. E. E Maslin, A. L. Rodgers, and W. G. F. Core, *Phys. Rev.* **164**, 1520 (1967).
72. R. Muller, A.A. Naqvi, F. Kappeler, and F. Dickmann, *Phys. Rev. C* **29**, 885 (1984).
73. A. S. Vorobyev and O. A. Shcherbakov, *Vopr. At. Nauki Tekh., Ser.: Yad. Reac. Konstanty*, No. 2, 52 (2016).
74. A. Trkov, R. Capote, and V.G. Pronyaev, *Nuclear Data Sheets* **123**, 8 (2015).
75. B. I. Starostov, V. N. Nefedov, and A. A. Boitsov, *Vopr. At. Nauki Tekh., Ser. Yad. Konst., No. 3*, 16 (1985).

Appendix 1

The main characteristic of the $^{235}\text{U}(\text{n}_{\text{th}},\text{f})$ fission fragments

Ref.	Method	$\langle m^*_L \rangle$	$\langle V^*_L \rangle$	$\langle V^*_H \rangle$	$\langle E^*_L \rangle$	$\langle \text{TKE} \rangle$
[1]	2v-2E, 2SSBD	95.93	1.423	0.977	100.6 ± 0.7	169.8 ± 0.8
[2]	2v	96.08	1.409	0.966	99.8 ± 1.0	168.3 ± 1.7
[3]	2v, 2SSBD	96.45	1.4203	0.9826	100.6 ± 0.3	170.36 ± 0.40
[4]	2v-2E, 2SSBD	95.87	1.415	0.97	99.08 ± 0.07	167.5 ± 0.2
[5]	2E-v	96.4	1.4223	0.9824	100.91 ± 0.2	170.6 ± 0.3
[6]	2E, 2SSBD	96.57			101.6 ± 1.0	171.9 ± 1.4
[7]	2E, 2SSBD	96.45			100.94 ± 0.4	170.7 ± 0.6
[8]	2E, 2SSBD	96.2			101.7 ± 1.5	172.0 ± 2.0
[9]	E-v, SSBD, PPAC	96.1			101.3 ± 1.0	171.1 ± 1.4
[10]	2E, 2SSBD	97.2			101.6 ± 0.3	172.9 ± 0.5
Average		96.3 ± 0.1			101.2 ± 0.4	171.0 ± 0.6
Recommended -V.G. Vorobyev, V.D. Kuzminov, VANT Ser. Nucl. Const. 1985, N2, p. 27						172.2 ± 0.4
Recommended (In book “The Nuclear fission process” Boca Raton, Florida, 1991, p. 323)						170.5 ± 0.5

- [1]. Y. Nakagome, I. Kanno and I. Kimura, “ $v(m^*)$ measurement for thermal neutron induced fission of ^{233}U and ^{235}U by double-velocity double-energy method”// In: H.D. Lemmel (Ed), Proc. IAEA Consult. Meeting, Vienna, INDC (NDS)-220, 1989, p. 65.
- [2]. J.C.D. Milton, J.S. Fraser, “Time-of-Flight fission studies on ^{233}U , ^{235}U and ^{239}Pu ” // *Can. J. Phys.*, 40, 1626 (1962).
- [3]. P. Geltenbort, F. Gonnenwein and A. Oed, “Precision measurements of mean kinetic energy release in thermal-neutron-induced fission of ^{233}U , ^{235}U and ^{239}Pu ” // *Radiat. Effects*, 93, 57 (1986).
- [4]. G. Andritsopoulos, “Correlated mass and energy distributions of fission fragments from ^{235}U by simultaneous velocity and energy measurements” // *Nucl. Phys.*, A94, 537-549 (1967).
- [5]. B. Hering and R. Muller, “Correlated mass and energy distributions of fission fragments from ^{235}U by simultaneous velocity and energy measurements” // *Nucl. Instr. Meth.*, 153, 235-238 (1978).
- [6]. H.W. Schmitt, J.N. Neilier and F.J. Walter, “Fragment energy correlation measurements for ^{252}Cf spontaneous fission and ^{235}U thermal-neutron fission” // *Phys. Rev.*, 141, 1146-1160 (1966).
- [7]. E. Weissenberger, P. Geltenbort, A. Oed, F. Gonnenwein, H. Faust, “Energy calibration of surface barrier detectors for fission fragments” // *Nucl. Instr. Meth.*, A248, 505-515 (1986).
- [8]. M.J. Bennett and W.E. Stein, “Kinetic energy of fragments from seven fission reaction at low excitation energies” // *Phys. Rev.*, 156, 1277-1282 (1967).
- [9]. K. Nishio, Y. Nakagome, H. Yamamoto, I. Kimura “Multiplicity and energy of neutrons from $^{235}\text{U}(\text{n}_{\text{th}},\text{f})$ fission fragments” // *Nucl. Phys.*, A632, 540-558 (1998).
- [10]. M. Asghar, F. Caitucoli, P. Perrin and C. Wagemans, “Fission fragment energy correlation measurements for the thermal neutron fission of ^{239}Pu and ^{235}U ” // *Nucl. Phys.*, A311, 205-218 (1978).

Appendix 2

The main characteristic of the $^{233}\text{U}(\text{n}_{\text{th}},\text{f})$ fission fragments

Ref.	Method	$\langle m^*_L \rangle$	$\langle V^*_L \rangle$	$\langle V^*_H \rangle$	$\langle E^*_L \rangle$	$\langle \text{TKE} \rangle$
[1]	2v-2E, 2SSBD	94.36	1.44	0.975	101.38 ± 1.0	170.16 ± 0.8
[2]	2v	94.57	1.442	0.963	99.9 ± 1.0	167.8 ± 1.7
[3]	2v, 2SSBD	94.91	1.4342	0.9793	100.90 ± 0.3	169.98 ± 0.40
[4]	2E, 2SSBD	94.8			101.7 ± 1.5	171.2 ± 2.0
[5]	E-v, SSBD, PPAC	95.5			101.7 ± 1.0	172.1 ± 1.4
[6]	2E, 2SSBD	94.84			101.9 ± 0.3	172.3 ± 0.5
Average		94.7 ± 0.2			101.5 ± 0.3	170.5 ± 0.5
Recommended -V.G. Vorobyev, V.D. Kuzminov, VANT Ser. Nucl. Const. 1985, N2, p. 27						171.5 ± 0.3
Recommended (In book “The Nuclear fission process” Boca Raton, Florida, 1991, p. 323)						170.1 ± 0.5

- [1]. Y. Nakagome, I. Kanno and I. Kimura, “ $v(m^*)$ measurement for thermal neutron induced fission of ^{233}U and ^{235}U by double-velocity double-energy method”// In: H.D. Lemmel (Ed), Proc. IAEA Consult. Meeting, Vienna, INDC (NDS)-220, 1989, p. 65.
- [2]. J.C.D. Milton, J.S. Fraser, “Time-of-Flight fission studies on ^{233}U , ^{235}U and ^{239}Pu ” // *Can. J. Phys.*, 40, 1626 (1962).
- [3]. P. Geltenbort, F. Gonnemann and A. Oed, “Precision measurements of mean kinetic energy release in thermal-neutron-induced fission of ^{233}U , ^{235}U and ^{239}Pu ” // *Radiat. Effects*, 93, 57 (1986).
- [4]. M.J. Bennett and W.E. Stein, “Kinetic energy of fragments from seven fission reaction at low excitation energies” // *Phys. Rev.*, 156, 1277-1282 (1967).
- [5]. K. Nishio, M. Nakashima, I. Kimura and Y. Nakagome, “Multi-parametric measurement of prompt neutrons and fission fragments for $^{233}\text{U}(\text{n}_{\text{th}},\text{f})$ ” // *J. Nucl. Sci. Tech.*, 35, 631-642 (1998).
- [6]. M. Asghar, F. Caitucoli, B. Leroux, P. Perrin and G. Barreau, “Fission fragment energy correlation measurements for $(\text{n}_{\text{th}}, \text{f})$ of ^{232}U and ^{233}U ” // *Nucl. Phys.*, A368, 328-336 (1981).

Appendix 3

The main characteristic of the $^{252}\text{Cf}(\text{sf})$ fission fragments

Ref.	Method	$\langle m^*_L \rangle$	$\langle V^*_L \rangle$	$\langle V^*_H \rangle$	$\langle E^*_L \rangle$	$\langle \text{TKE} \rangle$
[1]	2v	108.39	1.375	1.036	105.7 ± 1.1	185.7 ± 1.8
[2]	2v	108.25	1.370	1.034	105.7 ± 1.0	185.3 ± 1.7
[3]	2v	108.46	1.370	1.036	105.1 ± 1.0	184.9 ± 2.0
[4]	2E, 2SSBD	108.55			106.2 ± 0.7	186.5 ± 1.2
[5]	2E, 2SSBD	109.0			106.3 ± 0.7	187.3 ± 1.7
[6]	2E, 2SSBD	108.2			105.1 ± 1.5	184.3 ± 2.0
[7]	2E, 2SSBD	108.55			105.9 ± 0.7	186.2 ± 1.2
[8]	2E, 2SSBD	108.6			105.5 ± 0.6	185.8 ± 1.0
Average		108.5 ± 0.1			105.5 ± 0.6	185.3 ± 0.9
Recommended -V.G. Vorobyev, V.D. Kuzminov, VANT Ser. Nucl. Const. 1985, N2, p. 27						186.3 ± 1.0
Recommended (In book “The Nuclear fission process” Boca Raton, Florida, 1991, p. 323)						184.1 ± 1.3

- [1]. S.L. Whetstone, Jr. “Coincident time-of-flight measurements of the velocities of ^{252}Cf fission fragments” // *Phys. Rev.*, 131, 1232-1243 (1963).
- [2]. J.S. Fraser, J.C.D. Milton, H.R. Bowman and S.G. Thompson “” // *Can. J. Phys.*, 41, 2080 (1963).
- [3]. Yu.A. Barashkov et al, “TOF measurements of the corresponding fission fragments in spontaneous fission of Cm-244 and Cf-252” // *Yad. Fiz.* 13(6), 1162 (1971) (in Russian).
- [4]. H.W. Schmitt, J.N. Neilier and F.J. Walter, “Fragment energy correlation measurements for ^{252}Cf spontaneous fission and ^{235}U thermal-neutron fission” // *Phys. Rev.*, 141, 1146-1160 (1966).
- [5]. A. Gavron and Z. Fraenkel “Neutron correlations in spontaneous fission of ^{252}Cf ” // *Phys. Rev.*, C9, 632-645 (1974).
- [6]. M.J. Bennett and W.E. Stein, “Kinetic energy of fragments from seven fission reaction at low excitation energies” // *Phys. Rev.*, 156, 1277-1282 (1967).
- [7]. R. Schmidt and H. Henschel “Comparison of the spontaneous fission of ^{244}Cm and ^{252}Cf : (I). Fragment masses and kinetic energies” // *Nucl. Phys.*, A395, 15-28 (1983).
- [8]. G. Barreau, A. Sicre, F. Caitucoli, M. Asghar, T.P. Doan, B. Leroux, G. Martinez and T. Benfoughal, “Fission-fragment energy correlation measurements for $^{252}\text{Cf}(\text{sf})$ and structure in far-out asymmetric fission” // *Nucl. Phys.*, A432, 411-420 (1985).

Nuclear Data Section
International Atomic Energy Agency
Vienna International Centre, P.O. Box 100
A-1400 Vienna, Austria

E-mail: nds.contact-point@iaea.org
Fax: (43-1) 26007
Telephone: (43-1) 2600 21725
Web: <http://nds.iaea.org>
